ACS Catalysis

pubs.acs.org/acscatalysis

Research Article

Assessing a Photocatalytic Activity Index for TiO_2 Colloids by Controlled Periodic Illumination

Marco Prozzi,* Fabrizio Sordello, Simone Barletta, Marco Zangirolami, Francesco Pellegrino,* Alessandra Bianco Prevot, and Valter Maurino

Cite This: *ACS Catal.* 2020, 10, 9612–9623

Read Online

ACCESS | Metrics & More | Article Recommendations | Supporting Information

ABSTRACT: We demonstrated that controlled periodic illumination (CPI) is unable to increase the quantum yield (or photoefficiency) of the photocatalytic process. Nevertheless, choosing the appropriate experimental conditions and the use of CPI coupled with a simplified kinetic model allowed us to extract the lifetime of the species involved in substrate oxidation. These figures are usually elusive, even though there is a wide collection of hypotheses, guesses, and speculations in the literature. From our analysis, we defined a surface photocatalytic activity index. The latter consists of the ratio between the surface-defined kinetic constant for substrate oxidation and surface recombination and is independent of other experimental conditions, such as irradiance and catalyst concentration.

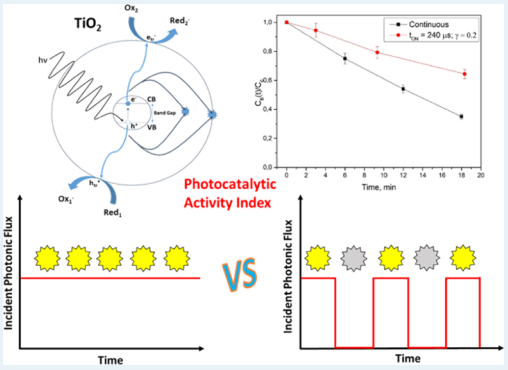

KEYWORDS: *controlled periodic illumination, TiO_2 photocatalysis, photoreactors, kinetic modeling, photocatalytic activity index*

1. INTRODUCTION

Over the years, the TiO_2 photocatalytic conversion of organic compounds proved to be one of the most promising ways for air and water remediation.[1] The low quantum yield of the photocatalytic processes is one of the many drawbacks for the wide use of this technology in the removal of pollutants from various environmental matrices.[2,3] Controlled periodic illumination (CPI) was investigated, in the field of TiO_2 photocatalysis, as a strategy to improve the performance of the process in the early nineties.[4] In Szechowski's seminal paper, the time profile of the photonic flux incident on a reaction cell during a CPI experiment consisted of a square wave, as depicted in Figure 1.

The square wave was identified by the specification of three different parameters: (1) I_0^{CPI} (mol s^{-1} cm^{-2}), which represents the constant photonic flux incident on the reaction cell during the light period (t_{ON}), (2) the period (P) which is the sum of the light and dark time ($P = t_{ON} + t_{OFF}$), and (3) the duty cycle (γ) is the fraction of the period in which the reaction cell is exposed to the constant photonic flux of the light source [$\gamma = t_{ON}/(t_{ON} + t_{OFF})$]. The alternating light and dark times depicted in Figure 1 were obtained originally employing an open channel reactor and wrapping sections of the light bulb with aluminum foil.[4] In recent years, the enormous progresses in light-emitting diode (LED) lifetime,[5] illumination efficiency, and total lumen output coupled with the possibility of electronically controlling their time profile emission up to a microsecond timescale accounted these sources more effective for CPI than for incandescent lamps

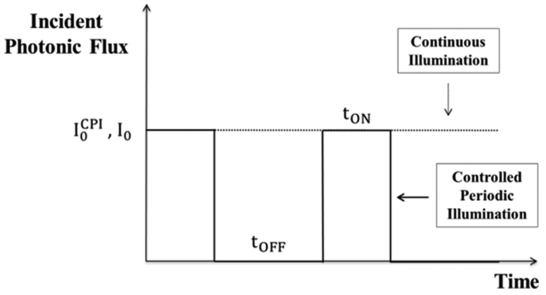

Figure 1. Intensity (incident photonic flux) vs time during a CPI experiment. I_0^{CPI} is the incident photonic flux during the light time (t_{ON}) of the CPI experiment, while t_{OFF} is the dark time. The constant photonic flux incident on the reaction cell during a continuous illumination experiment (I_0) is represented with the dashed line.

that cannot be turned on and off alternately in a similar timescale, therefore, requiring the use of complex mechanical shutters.[6] Only in the case of the LED sources, there is an equivalence between the shape of the photonic flux incident on the reaction cell and the time profile emission of the irradiation

Received: June 8, 2020
Revised: July 25, 2020
Published: July 27, 2020

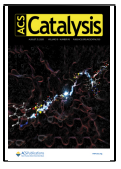

https://dx.doi.org/10.1021/acscatal.0c02518
ACS Catal. 2020, 10, 9612–9623

system: this aspect is extremely important if an alleged enhancement of the quantum yield due to the CPI technique must be associated with a reduction in electrical power consumption for pollutant abatement. Through the comparison of continuous and CPI experiments at the $I_0 = I_0^{CPI}$, Sczechowski and co-workers reported a fivefold increase in the photoefficiency for formate ion oxidation in concentrated TiO_2 aqueous slurries.[4] A subsequent study under similar conditions (TiO_2 aqueous slurry and formic acid) indicated that, by comparing continuous versus CPI experiments in which $I_0 = \gamma I_0^{CPI}$, there is no quantum yield (or photoefficiency) enhancement due to the CPI technique.[7] The dependence of the TiO_2 photocatalytic degradation rate (or quantum yield/photoefficiency) on the duty cycle, period, and light/dark times has been observed in CPI studies both for gas−solid and liquid−solid experiments.[7−9] The Langmuir−Hinshelwood CPI rate model proposed by Chen et al.[6] incorporates the duty cycle in the well-known Langmuir−Hinshelwood model to predict the reaction rate under CPI conditions; however, it did not accurately predict the photocatalytic decomposition of methyl orange under periodic illumination.[10] The vast majority of studies investigating CPI have relied on this experimental approach.[11] Both quantum yield-based models and photocatalytic rate models were used for the interpretation of CPI experimental data and to understand the phenomena that occur in the semiconductor catalyst during CPI.[10] In this paper, we proposed a simplified kinetic model that allowed us both to evaluate if the CPI technique is able to improve the catalyst performances and to extract intrinsic kinetic parameters of the TiO_2 photocatalytic system that affect the catalyst activity by the coupling of a very restricted number of continuous and periodic illumination experiments. In order to do this, we use formic acid as the substrate, a simple pollutant mainly released by the paper industry.[12]

2. EXPERIMENTAL SECTION

2.1. Reagents and Materials. Formic acid (>98%), $HClO_4$ (70% w/w), and K_2CO_3 (>99%) were purchased from Sigma-Aldrich. Titanium dioxide Evonik P25 (85% anatase/15% rutile; Evonik Industries AG, Essen, Germany) has a Brunauer−Emmett−Teller specific surface area of 55 $m^2\ g^{-1}$. Before usage, a photocatalyst suspension was cleaned by dialysis against Milli-Q grade water in order to remove inorganic ions that could affect the degradation.[13] Finally, the suspension was frozen and freeze-dried to obtain a cleaned powder without any heat treatment. The water used in the experiments was of Milli-Q quality. The suspensions, sonicated for 20 min with a Branson CPX ultrasonic bath before each photocatalytic test, were prepared in aqueous solution of 3×10^{-4} M of $HClO_4$ to fix the pH value considerably lower than pH_{PZC} to stabilize the catalyst colloids during the irradiation experiments.[14,15]

2.2. Irradiation Experiments. Irradiation experiments were performed in a bench-scale photoreactor (Figure 2).

The LED source is equipped with two UV 360 nm LEDs (model LZ1-00UV00-0100) mounted on a printed circuit, whose irradiance is controlled through a control software written in LabVIEW 2015 SP1, varying the current flowing in the LEDs. The radiation was filtered with one 3.3 mm thick frosted borosilicate glasses in order to obtain a uniform diffuse radiation. The LED source's emission is set by a function generator built with a digital-analogic converter (AD/DA converter model number PCIe-6353, National Instruments, https://www.ni.com/it-it/support/model.pcie-6353.html).

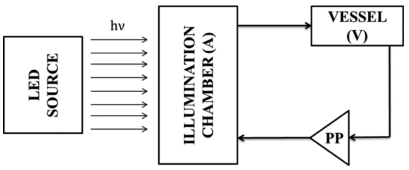

Figure 2. Photoreactor used for the photocatalytic tests. PP denotes the peristaltic pump.

The electrical scheme of the LED source and a picture of the printed circuit are reported in the Supporting Information (see Figures S3 and S4, respectively). For CPI experiments, the software requires the specification of the period (P) and duty cycle (γ); continuous illumination experiments are performed placing duty cycle equal to one. Because the irradiance of the LED sources depends on the temperature, we used a thermostating system with two Peltier's cells, two cooling fans, and a two-value proportional−integral−derivative control to minimize temperature excursions during irradiation experiments. The correspondence between the software-constructed square wave and the actual emission of the source has been verified for every experimental condition with an oscilloscope (Tektronix TDS 1012) and a photodiode (for the electrical scheme of the photodiode, see Figure S5 in the Supporting Information): for the unique duty cycle we used in this work for CPI experiments (γ = 0.2), the irradiation system was able to provide square wave light pulses with the width from 100 μs to 240 ms (Figure S6 in the Supporting Information reported some examples of the actual emission of the LED source for various t_{ON}). For continuous illumination experiments, we determined the incident photonic flux at the top of the slurry (I_0) by mediating on the surface of the illumination chamber (filled with water) the irradiance value (W m^{-2}) provided by a CO.FO.ME.GRA (Milan, Italy) power meter in the range 290−400 nm and assuming that LED emission is monochromatic at the wavelength where the maximum (λ_{max} = 370 nm) is located. The normalized spectrum of the UV-LED (I/I_{max} vs λ) is reported in Figure S7 in the Supporting Information. During every CPI experiment, the incident photonic flux at the top of the slurry ($=I_0^{CPI}$) was $4.09 \pm 0.1 \times 10^{-8}$ mol s^{-1} cm^{-2} (i.e., the maximum value among the I_0 for the continuous illumination experiments): we checked that the peak voltage value recorded by the oscilloscope (for every t_{ON} employed) was the same as that observed for continuous irradiation of the photodiode at $I_0 = 4.09 \pm 0.1 \times 10^{-8}$ mol s^{-1} cm^{-2}. During t_{OFF}, the voltage value recorded is equal to that measured when the photodiode is kept in the dark. The illumination chamber (Figure 2) represents the portion of the photoreactor in which the photocatalytic slurry is irradiated. The basic structure is made of polyoxomethylene (POM). Figure 3b shows the internal section of the chamber, where the fluid distributor and the UV-transparent glass housing are highlighted. The area of the illumination chamber is A_{IC} = 43.3 cm^2. This figure is larger than the value calculated from the data reported in the Supporting Information (Figure S9c). Indeed, A_{IC} does not represent the area from which the radiation enters the illumination chamber, but it is the entire illuminated area of the illumination chamber. In fact, in the small lateral portion not directly irradiated by the LED source, the radiation is provided by scattering phenomena. However, we used the value calculated from Figure S9c in the quantum yield evaluation. The volume of the illumination chamber is a function of the spacer adopted (i.e., the volume of the suspension contained in

https://dx.doi.org/10.1021/acscatal.0c02518
ACS Catal. 2020, 10, 9612−9623

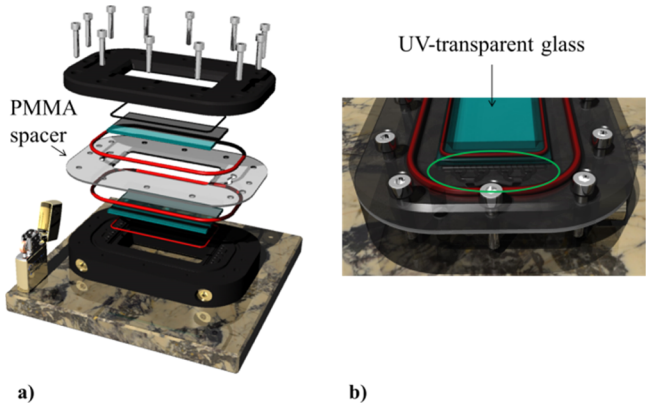

Figure 3. (a) Disassembled components of the illumination chamber: four O-rings (red) are employed to avoid leaks from the chamber; the two basic POM structures (black) and the PMMA spacer are closed with 12 screws. (b) Focus on the internal section of the illumination chamber where the fluid distributor (green circle) and the UV-transparent glass housing are highlighted.

the chamber = $V_A = A_{IC} \cdot b$): in this work, we used two different spacers with thicknesses of 1 and 3 mm, respectively. The spacer is entirely made of polymethylmethacrylate (PMMA). Other schemes, a picture of the illumination chamber, and some pictures of the photoreactor during an irradiation experiment are reported in the Supporting Information (see Figures S9, S8, and S1, S2 respectively).

The vessel (V), made of PMMA, is a fraction of the total part of the photoreactor where the photocatalyst suspension is kept in the dark. The suspension contained in the vessel is continually stirred. In the text, we refer to the volume of suspension contained in the vessel with the notation V_V. The peristaltic pump (PP) was able to provide a volumetric flow rate from about 17 to nearly 95 mL min^{-1}: the volume of the pipes (made of Teflon) and that of the inner hydraulic circuit of the PP are denoted with V_M, and it represents another part of the reactor where the photocatalyst suspension is not irradiated. All the experiments were performed in the following conditions:

- Substrate: formic acid (HCOOH), initial concentration $C_0 = 2 \times 10^{-4}$ M;
- Photocatalyst: titanium dioxide Evonik P25, $C_{Cat} = 0.1$ g L^{-1};
- pH = 3.5 by perchloric acid;
- Ambient air and room temperature.

Before each photocatalytic test, the suspension loaded in the photoreactor underwent a conditioning step, in which it was recirculated for 20 min with the LED source at an irradiance of 130 W m^{-2}. Subsequently, it is discharged into the vessel, and the substrate is added to the suspension. After 10 min of stirring in the dark, the suspension is recirculated for 3 min in the entire photoreactor (with the LED source turned off) to have the substrate concentration uniform in every part of the photoreactor before irradiation begins. At established time intervals, samples were collected from the vessel with a syringe (0.5−1 mL per sample) and filtered through 0.45 μm membranes [poly(vinylidene difluoride), Sigma-Aldrich]. For the "zero-time" of the experiment, we measured a significant difference (10−15%) between analytical (calculated) concentration and measured value due to the adsorption on the catalyst surface. Even though other substrates are less prone to adsorption, we chose formic acid to avoid the formation of intermediates during the degradation process.[7]

2.3. Analytical Determinations. The evolution of the substrate concentration as a function of time is monitored with ion chromatography. Both formate standard solutions and samples were analyzed using a Dionex DX 500 instrument equipped with an ED40 conductibility detector, an LC30 chromatography oven, a GP40 pump, an AS9-HC ion exchange column (250 mm × 4 mm i.d.), an ION PAC AG9-HC precolumn, and an ASRS-ULTRA 4 mm suppressor. Formate ion was eluted with a Milli-Q solution of K_2CO_3 (9 mM), with a flow rate of 1 mL min^{-1}, and with an SRS current of 100 mA. Under these conditions, the retention time for formate is 4.1 min.

2.4. Kinetic Model. The complexity of the photocatalytic process is both related to the heterogeneity and multiplicity of the phenomena that occur during substrate degradation and the great number of experimental variables that can influence the observed rate. The scheme of the primary steps of the photocatalytic process is represented in Figure 4.

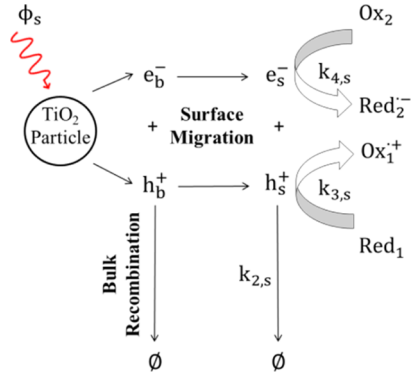

Figure 4. Primary steps of the photocatalytic process (Minero and Vione[16]). ϕ_s (mol s^{-1} m^{-2}) is the rate of radiation absorption per unit surface area of the catalyst; e_b^- and h_b^+ are, respectively, the photogenerated electrons and holes in the semiconductor bulk; e_s^- and h_s^+ are the species resulting from the surface trapping of electron and holes on the surface of the catalyst. $k_{2,s}$, $k_{3,s}$, $k_{4,s}$ (m^2 mol^{-1} s^{-1}) are, respectively, the surface-defined kinetic constants for surface recombination, substrate (Red_1) oxidation by h_s^+, and oxidant (Ox_2) reduction by e_s^-; ⌀ represents the heat resulting from the recombination processes that can occur both in the bulk and at the surface of the semiconductor. Back reactions are neglected.

The absorption of light with $h\nu \geq E_{bg}$ and the subsequent charge separation produce initially equivalent bulk concentration of charge carriers, e_b^-, h_b^+. The photogenerated charge carriers that reach the surface of the catalyst (e_s^-, h_s^+) can recombine on surface traps or undergo interfacial electron transfer with the adsorbed reduced species Red_1 (the substrate) and the oxidant Ox_2. Both bulk and surface recombination limit the quantum yield of the photocatalytic process.[16] The development of quantitative kinetic models that take into account the totality of the processes involved in the photocatalytic system is practically impossible. Consequently, simplifying assumptions are required to obtain an analytical function that establish a cause—effect relationship among traditional aqueous slurry experimental variables. According to Minero and Vione,[16] the photogenerated surface species are considered indistinguishable: so, the notations e_s^- and h_s^+ sum up all photogenerated reactive species, in which e_s^- can be

https://dx.doi.org/10.1021/acscatal.0c02518
ACS Catal. 2020, 10, 9612−9623

considered as an electron in the conduction band or a trapped electron in a titanium center of the lattice, whereas h_s^+ denotes a hole in the valence band, a trapped hole localized in the oxygen atom of the lattice or a surface-bonded hydroxyl radical. Furthermore, on applying the steady-state approximation to bulk electron and hole concentration and considering that the bulk recombination is an unfavorable process for TiO_2, the system of differential equations for the surface electron and hole concentration is directly derived from Figure 4[16]

$$\frac{d\{e_s^-\}}{dt} = \phi_s - k_{2,s}\{e_s^-\}\{h_s^+\} - k_{4,s}\{e_s^-\}\{Ox_2\}$$

$$\frac{d\{h_s^+\}}{dt} = \phi_s - k_{2,s}\{e_s^-\}\{h_s^+\} - k_{3,s}\{h_s^+\}\{Red_1\}$$

where ϕ_s (mol s^{-1} m^{-2}) is the rate of radiation absorption per unit surface area of the catalyst; $k_{2,s}$, $k_{3,s}$, $k_{4,s}$ (m^2 mol^{-1} s^{-1}) are, respectively, the surface-defined kinetic constants for surface recombination, substrate oxidation, and oxidant reduction, and the notation $\{i\}$ indicates the surface concentration of species "i" (mol m^{-2}). From the analysis of these equations, we infer that there are three different contributions in determining the time evolution of charge carrier concentration and, for the continuous illumination, the steady state value. However, if the irradiation experiments are carried out at very low reductant/oxidant volume concentration (ideally $[Red_1]$, $[Ox_2] \rightarrow 0$), we can clearly overlook the change in charge carriers concentrations caused by interfacial electron transfer with the adsorbed molecules on the catalyst surface. In the latter case (*recombination regime*), the nontrivial solution can be obtained solely based on the assumption that surface concentrations of positive and negative charge carriers are equivalent ($\{e_s^-\} = \{h_s^+\}$). Consequently, in the *recombination regime*, the differential equation that describes surface concentration of h_s^+ becomes

$$\frac{d\{h_s^+\}}{dt} = \phi_s - k_{2,s}\{h_s^+\}^2 \quad (1)$$

2.5. Degradation Rate under Continuous Illumination. Under constant lighting conditions, the surface concentration of charge carriers will reach the steady state value (subscript "ss"), which is equal to $\{h_s^+\}_{ss} = \phi_s/k_{2,s}$. Taking into account that:

(1) photocatalytic reactions occur at the surface of the catalyst;[2,17]
(2) it is possible to employ Langmuir's isotherm to describe the partitioning of Red_1 between the photocatalyst surface and the bulk solution,[18] with specific substrate adsorption sites;[3,19]
(3) although Brandi et al.[20,21] have shown that in practical systems, the distribution of radiation intensities inside the reactor space is highly nonuniform and have proposed the use of the radiative transfer equation to assess the local volumetric rate of photon absorption, we decided to employ the Kubelka–Munk function (KM), because Minero and co-workers elegantly demonstrated that it is able to describe the absorption and scattering phenomena for aqueous TiO_2 slurries very well.[16,18]

Therefore, in the case of zero-order kinetics toward aqueous substrate concentration (which is the regime experimentally observed), the rate of aqueous substrate removal from the irradiated suspension volume (i.e., the *intrinsic degradation rate* in M s^{-1}) is equal to

$$k_{Deg} = k_{3,s}\sigma_s'\left[\sqrt{\frac{10^3 k I_0 C_{Cat} S}{k_{2,s}}}\,\frac{1}{b}\int_0^b \sqrt{T(z)}\,dz\right] \quad (2)$$

where σ_s' (mol m^{-2}) indicates the moles of substrate adsorption sites per unit surface area of the catalyst, I_0 (mol s^{-1} cm^{-2}) is the photonic flux incident on the reaction cell, C_{Cat} (g L^{-1}) is the photocatalyst loading, k (cm^{-1}) is the (C_{Cat} dependent) absorption coefficient of the suspension according to the KM model,[16,18] S (m^2 g^{-1}) is the photocatalyst specific surface area, $T(z)$ is the transmittance of the suspension at a distance z from its top, and b (cm) is the thickness of the irradiated suspension. In the development of the kinetic model, the terms σ_s', k, C_{Cat}, S, and $T(z)$ have been considered constant over the time because the condition pH much lower than pH_{PZC} (see paragraph Section 2.1) prevents agglomeration and sedimentation processes. We monitored both pH and $T(b)$ during the photodegradation without noting remarkable differences between the beginning and the end of the experiments. Therefore, k_{Deg} is also constant over the time. The term contained in square brackets of eq 2 consists of the average volumetric concentration of the active oxidizing species over the irradiated suspension volume in a steady-state condition (i.e., the ratio between the moles of h_s^+ in the irradiated volume under the steady state condition and the entire irradiated volume): consequently, we can formally express the degradation rate of aqueous substrate as

$$k_{Deg} = k_{3,v}[h_s^+]_{ss} \quad (3)$$

where $k_{3,v}$ (s^{-1}) = $k_{3,s}$ σ_s' is the kinetic constant for substrate oxidation defined over the entire irradiated volume. The introduction of a dimensionless corrective factor $\psi = \frac{\left[\int_0^b \sqrt{T(z)}\,dz\right]^2}{b\int_0^b T(z)\,dz}$, which is very close to unity for the operating adopted conditions (see the "Results and Discussion" section for the experimental procedure employed for its estimation), allows us to write

$$[h_s^+]_{ss} = \sqrt{\overline{\phi_V}/k_{2,v}} \quad (4)$$

where $k_{2,v}$ (M^{-1} s^{-1}) = $k_{2,s}/(C_{Cat}S)$ is the kinetic constant for surface recombination defined over the entire irradiated volume and $\overline{\phi_V}$ (mol s^{-1} L^{-1}) is the average photonic flow absorbed per volumetric unit of suspension (i.e., the ratio between the moles of the photon absorbed per unit time in the irradiated suspension volume and the entire irradiated suspension volume). Equation 4 is the steady-state solution of the following differential equation

$$\frac{d[h_s^+]}{dt} = \overline{\phi_V} - k_{2,v}[h_s^+]^2 \quad (5)$$

which is the homologous of eq 1, but expressed in terms of average volumetric variables.

2.6. Degradation Rate under CPI. The quantitative description of the photocatalytic system under CPI conditions is essentially inspired by the theory of intermittent illumination developed in 1945.[22−24] To obtain the expression for the substrate degradation rate under CPI, it is necessary to separately solve the differential equations that describe the concentration of the charge carriers (considering the system always in the *recombination regime*) during

https://dx.doi.org/10.1021/acscatal.0c02518
ACS Catal. 2020, 10, 9612−9623

$$\text{light time } (t_{ON}) \rightarrow \frac{d[h_s^+]}{dt} = \overline{\phi_V} - k_{2,v}[h_s^+]^2$$

and

$$\text{dark time } (t_{OFF}) \rightarrow \frac{d[h_s^+]}{dt} = -k_{2,v}[h_s^+]^2$$

The resolution is carried out assuming that, in the various light and dark cycles, the charge carrier concentration always fluctuates between two precise extremes. The numeric values of these extremes are constant over the time of the irradiation experiment (*two-value condition*). In other words, it is assumed that the photocatalytic system responds to the periodicity of the lighting with an intrinsic periodicity, which is related both to operating conditions (γ, t_{ON}) and properties of the catalyst ($k_{2,v}$). When $I_0^{CPI} = I_0$, the ratio between the aqueous degradation rate under CPI (k_{Deg}^{CPI}) and the aqueous degradation rate under continuous illumination (k_{Deg}) results

$$\frac{k_{Deg}^{CPI}}{k_{Deg}} = (1+r)^{-1}\left\{1 + m^{-1}\ln\left[1 + \frac{rm}{1 + ([h_s^+]_2/[h_s^+]_{ss})^{-1}}\right]\right\}$$

with

$$\frac{[h_s^+]_2}{[h_s^+]_{ss}} = \frac{rm\tanh(m) + \sqrt{[rm\tanh(m)]^2 + 4[rm + \tanh(m)]\tanh(m)}}{2[rm + \tanh(m)]} \quad (6)$$

where tanh is the hyperbolic tangent function, $r = \gamma^{-1}(1-\gamma)$, ${h_s^+}_2$ (M) is the volumetric concentration of the charge carriers at the end of the light flash and $m = t_{ON}/\tau_L$, in which

$$\tau_L = \sqrt{(k_{2,v}\overline{\phi_V})^{-1}} \quad (7)$$

is the time required (for the recombination process) to remove, from the irradiated suspension volume, a number of moles of charge carriers equivalent to those present in the steady-state condition under continuous illumination for an incident photonic flux equal to I_0. Therefore, in addition to continuous illumination experiments, under CPI, there are two more parameters that can affect the observed degradation rate. The former is the duty cycle (γ), as previously mentioned in the Introduction. Indeed, for a photochemical process, until the diffusion control is reached, a change in the average photon flux determines a variation in the rate of reaction.[25] The latter is t_{ON}. Apart from what has been observed in the field of TiO_2 photocatalysis,[7−9] the influence of t_{ON} on a photochemical process was first experimentally noted in the early 1920s by Berthoud and Bellenot[26] for the photochemical reaction between bromine/iodine with potassium oxalate, a process in which the reaction rate is a function of the square root of the incident light intensity. The theory of intermittent illumination has been later used for the analysis of polymerization and oxidation processes by various authors.[22−24,27−29] Starting from eq 6, we can show that, for a system in the *recombination regime*, the behavior of the photocatalyst is very different if t_{ON} is greater or minor compared with τ_L. Two different limiting behaviors will be observed

$$\lim_{m\to+\infty}\frac{k_{Deg}^{CPI}}{k_{Deg}} = \gamma \text{ and } \lim_{m\to 0}\frac{k_{Deg}^{CPI}}{k_{Deg}} = \sqrt{\gamma} \quad (8)$$

Therefore, on plotting the ratio between the rate under pulsed irradiation and under constant irradiation versus $\log_{10} t_{ON}$, an inverted logistic S-shaped curve is obtained because $0 < \gamma < 1$. A nonlinear regression procedure has been used to experimentally estimate the lifetime of the active oxidizing species (τ_L).

2.7. Evaluation of Kinetic Parameters. From the observation of Figure 2, it is evident that the photocatalyst slurry is subjected to a periodic illumination even when the irradiance of the LED source is kept constant during the time ($\gamma = 1$) because the PP recirculates the suspension between the illumination chamber (A) and the vessel (V). The samplings are performed from the vessel, so it is necessary to obtain a relationship that expresses the time profile of substrate concentration in the vessel as a function of the kinetic parameter (k_{Deg} or k_{Deg}^{CPI} for CPI experiments) and that of the parameters inherent to the operating conditions in which the photoreactor is used. First of all, we define: $C_A(t)$ and $C_B(t)$, the molar aqueous concentration of the substrate in the illumination chamber (subscript "A") and in the total part of the photoreactor which is not exposed to the LED source (subscript "B", B = V ∪ PP), respectively; so, $V_B = V_V + V_M$ is the total volume of the suspension which is in the dark portion of the photoreactor. V_{tot} is the total volume of suspension loaded in the photoreactor. From the mass balance for the substrate, we can also write the total concentration in the entire photoreactor as (subscript "tot")

$$C_{tot}(t) = \chi_A C_A(t) + \chi_B C_B(t) \quad (9)$$

where $\chi_A = V_A V_{tot}^{-1}$ and $\chi_B = V_B V_{tot}^{-1}$. To obtain treatable analytical solutions, we have to make three assumptions: (i) absence of spatial gradient concentration in the flow direction of the fluid inside the illumination chamber; (ii) constant flow over the time (i.e., we neglected the intrinsic intermittent PP flow and denoted the volumetric flow rate as F, mL min^{-1}); (iii) because for a degradation experiment, in addition to the "zero time", only three samples were collected [$5\% < \Delta V_B/V_B\ (t=0) < 11.5\%$]; we did not consider the changes in V_B and V_{tot} (and consequently in χ_A and χ_B) due to sampling. The system of differential equations written below (eq 10) takes into account all the processes that can change the substrate concentration in the two distinct parts of the photoreactor and assumes that: (1) the residence time of a volumetric element in the illumination chamber ($t_r = V_A F^{-1}$) is considerably greater than of the time required to achieve the steady-state condition for the concentration of the active oxidizing species (h_s^+) during continuous illumination experiments; (2) the residence time of a volumetric element in the portion "B" of the photoreactor ($t_r^B = V_B F^{-1}$) is much greater than τ_L. In other words, we assume that degradation of the substrate takes place in the illumination chamber only and also in the steady-state condition for $[h_s^+]$ during continuous illumination experiments.

$$\frac{d(C_A)}{dt} = -k_{Deg} + \frac{F}{V_A}[C_B - C_A]$$

$$\frac{d(C_B)}{dt} = -\frac{F}{V_B}[C_B - C_A] \quad (10)$$

Differentiating with respect to time eq 9 and substituting the expression above reported for $d(C_A)/dt$ and $d(C_B)/dt$ (eq 10), we obtain: $d(C_{tot})/dt = -k_{Deg}\chi_A$; on placing $k_{obs} = k_{Deg}\chi_A$ and using the initial condition $C_{tot}(0) = C_0$, we can integrate the differential equation for C_{tot} to obtain

$$C_{tot}(t) = C_0 - k_{obs}t \quad (11)$$

https://dx.doi.org/10.1021/acscatal.0c02518
ACS Catal. 2020, 10, 9612−9623

Moreover, starting from eq 9, we can write $C_A = \chi_A^{-1}[C_{tot} - \chi_B C_B]$: introducing this into the differential equation for C_B (eq 10) and using the expression of eq 11 for C_{tot}, it follows that

$$\frac{d[C_B - C_0]}{dt} = -q[C_B - C_0] - qk_{obs}t \quad (12)$$

where $q\ (min^{-1}) = F/V_B\chi_A$. The general analytical solution of eq 12 is: $C_B(t) - C_0 = g(t)e^{-qt}$ with $g(t) = -qk_{obs}\int t\, e^{qt}\, dt + c_1$, where c_1 is the integration constant. Using the initial condition $C_B(0) = C_0$, the expression that describes the time evolution of substrate concentration in the vessel (V ⊂ B) during the photocatalytic degradation is

$$C_B(t) = C_0 - k_{obs}\left\{t - \left[\frac{1}{q} - \frac{e^{-qt}}{q}\right]\right\} \quad (13)$$

Some examples for the formic acid degradation trends $\left(\frac{C_B(t)}{C_0}\text{ vs }t\right)$ are reported in the Supporting Information (Figures S10 and S11). The plot of $[C_0 - C_B(t)]$ versus $\left\{t - \left[\frac{1}{q} - \frac{e^{-qt}}{q}\right]\right\}$ gives the rate of aqueous substrate removal from the entire photoreactor (k_{obs}) as its slope and, from this, the *intrinsic degradation rate* k_{Deg} ($=k_{obs}\chi_A^{-1}$) is determined. It is always possible to fit the data because q contains parameters that are known to the operator (eq 12). The *observed degradation rate* is $-\frac{d(C_B)}{dt} = k_{obs}[1 - e^{-qt}]$: taking into account the q values for our experimental conditions (see "Results and Discussion"), it implies that $t \geq 45\text{ s} \rightarrow e^{-qt} < 0.05$ and so, k_{obs} can be reasonably considered also as the *observed degradation rate*. Equation 13 shows how the operating conditions in which the photoreactor is used may affect the time profile of substrate concentration in the vessel. However, while applying this equation to the fit of the experimental data, it must be remembered that this expression was obtained according to specific assumptions involving the residence time in the illumination chamber. In fact, if the flow (F) is too high, the residence time in the illumination chamber (t_r) is too short to achieve the steady state for $[h_s^+]$. Consequently, k_{obs} does not factor in the product of k_{Deg} and χ_A. On the other hand, if F is too low (and so t_r too high), it is possible that a concentration gradient is generated in the illumination chamber. In this case, we could not refer to that portion of the photoreactor (A) with a unique value for the substrate concentration (C_A), making the model conceptually wrong. Furthermore, there are interdependencies between the *intrinsic degradation rate* (k_{Deg}) and the photoactive fraction volume (χ_A) that should not be forgotten: the linear relationship between k_{obs} and χ_A turns out to be true only if the change in χ_A is caused by a variation in the total volume of suspension loaded in the photoreactor (V_{tot}): indeed, if the change in χ_A is obtained by adopting another spacer, there is also a change in the thickness of the irradiated suspension, and this is accompanied by a variation in k_{Deg} (eq 2). For each CPI experiment with $t_{ON} \leq 240$ ms, the value of k_{Deg}^{CPI} is obtained with the same procedure described above: the implicit assumption is that a volumetric element is subjected to a number of light and dark cycles inside the illumination chamber ($=t_rP^{-1}$) that is enough to achieve the *two-value condition*, which is one of the most important hypotheses employed to describe the photocatalytic system under CPI (Section 2.2).

3. RESULTS AND DISCUSSION

The simplest and fastest way to check the validity of the procedure developed to determine the k_{Deg} value starting from the $C_B(t)$ profile is to perform two continuous illumination experiments with the same spacer (b = 0.3 cm), the same incident photonic flux ($I_0 = 4.09 \times 10^{-8}$ mol s^{-1} cm^{-2}), and the same flow ($F \approx 50$ mL min^{-1}, from which $t_r \cong 16$ s), but different total volumes (V_{tot}). If the assumptions are correct, then the ratio between the measured k_{obs} values will be equal to the reciprocal of the ratio between the total volume of suspension loaded in the photoreactor in the two experiments $\left(\text{i. e. } \frac{k_{obs}(1)}{k_{obs}(2)} = \frac{V_{tot}(2)}{V_{tot}(1)}\right)$. For $V_{tot}(1)$ = 64.68 mL and $V_{tot}(2)$ = 33.25 mL, we obtained $k_{obs}(1) = (6.45 \pm 0.28) \times 10^{-8}$ M s^{-1} and $k_{obs}(2) = (1.18 \pm 0.08) \times 10^{-7}$ M s^{-1}, from which $k_{obs}(1)/k_{obs}(2) = 0.548 \pm 0.058$ and $V_{tot}(2)/V_{tot}(1) = 0.514$. The ratio between k_{obs} exceeded only by 6% of the theoretical prevision; we considered this discrepancy acceptable, and consequently, we decided to perform all the continuous illumination experiments with a residence time in the illumination chamber of about 16 s (or slightly higher) because for this t_r, the active species achieves steady state values for their volumetric concentration inside the illumination chamber. A direct implication of the *recombination regime* is the dependence of the *intrinsic degradation rate* (k_{Deg}) on the square root of the incident photonic flux (I_0) (eq 2). Because, as illustrated in Section 2.2, this aspect is of fundamental importance for kinetic modeling under CPI conditions, this relationship was verified by performing a series of experiments at different incident photonic fluxes. When the data are reported as a function of $\sqrt{I_0}$, we were able to highlight a linear relation with R^2 = 0.991 (Figure 5).

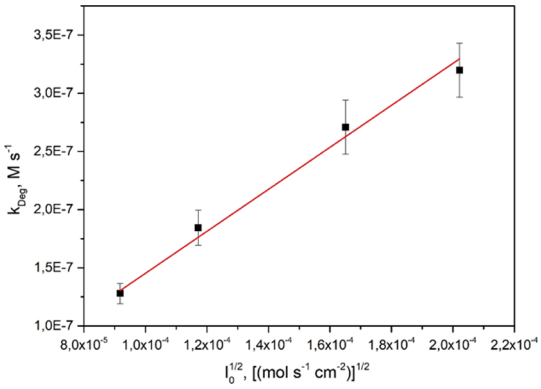

Figure 5. Intrinsic degradation rate (k_{Deg}) as a function of the square root of the photonic flux incident on the reaction cell (I_0). As required by the recombination regime hypothesis, k_{Deg} shows a linear dependence on the square root of I_0 with R^2 = 0.991. Each experiment was carried out with b = 0.3 cm, χ_A = 0.38, V_{tot} = 33.25 mL, and t_r = 17.8 s. Error bars account for one standard deviation.

In the Section 2.3 we developed a model to evaluate how the photoreactor can influence the observed degradation rate, assuming that there are not spatial gradients concentration in the illumination chamber. In other words, we have considered our photoreactor as a recirculating continuous stirred tank reactor (CSTR). We verified this hypothesis using the biggest k_{Deg} value observed (in the set of measures k_{Deg} vs I_0) and considering the photoreactor as a recirculating plug flow reactor (PFR): from this point of view, there will be a gradient concentration along the flow direction of the fluid inside the illumination chamber,

https://dx.doi.org/10.1021/acscatal.0c02518
ACS Catal. 2020, 10, 9612−9623

which is intuitively related to both k_{Deg} and t_r (for a useful comparison between CSTR and PFR, see ref 30). In the following discussion, $C_{In}(t)$ and $C_{Out}(t)$ are the time-dependent substrate concentration in the volumetric element at the entrance and at the outlet of the illumination chamber, respectively, as reported in Figure 6.

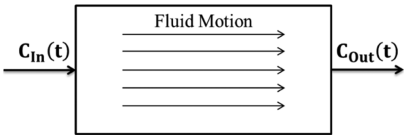

Figure 6. Schematic representation of the illumination chamber as a PFR. The substrate enters the illumination chamber at a concentration $C_{In}(t)$ and exits from it with a concentration $C_{Out}(t)$ ($<C_{In}(t)$) because of the photocatalytic degradation processes, in which it is involved for the time that it remains inside the chamber ($=t_r$).

The equality $C_{In}(t) = C_B(t)$ is true, so we can write the following expression

$$C_{In}(t) = C_0 - k_{obs}\left\{t - \left[\frac{1}{q} - \frac{e^{-qt}}{q}\right]\right\}$$

In the limit case of the PFR, we can state that $C_{Out}(t) = C_{In}(t - t_r) - k_{Deg}t_r$ and so

$$C_{Out}(t) = C_0 - k_{obs}\left\{t - \left[\frac{1}{q} - \frac{e^{qt_r}e^{-qt}}{q}\right]\right\} - k_{Deg}t_r\chi_B$$

It is important to pay attention to the fact that the goal of this discussion is to determine the difference of concentration *under the assumption that we may refer to the illumination chamber with a unique value for the substrate concentration*. If the calculated difference of concentration between entrance and outlet will be large, then we will have to discard this assumption, and we will not be able to employ the model developed in Section 2.3 to estimate the intrinsic degradation rate. Remembering that $k_{obs} = k_{Deg}\chi_A$, for $t \geq t_r$, the difference in concentration results in

$$C_{In}(t) - C_{Out}(t) = \frac{k_{Deg}}{q}\{1 + \chi_A[e^{qt_r} - 1]e^{-qt}\} \quad (14)$$

The term contained in brackets of eq 14 is the time-dependent component. Figure 7a shows that for the operating conditions in which the photoreactor is used, the value of such term quickly tends to unity.

For $t \geq 2.5t_r$ (≈45 s), it results in $\chi_A[e^{qt_r} - 1]e^{-qt} < 0.03$: this implies that in a very short time, if compared to the duration of the entire irradiation experiment (15−45 min), the concentration difference is no longer dependent on the irradiation time and is equal to

$$C_{In}(t) - C_{Out}(t) = \frac{k_{Deg}}{q} \quad (15)$$

To assume that the substrate concentration in the illumination chamber has a single value (C_A), the smallest $C_{Out}(t)$ should be equal to $0.9C_{In}(t)$. Therefore, the smallest observable value of $C_{In}(t)$ ($=C_B(t)$) during an irradiation experiment is

$$C_B(t) = 10\frac{k_{Deg}}{q}$$

The maximum value of k_{Deg} that we have recorded (in the set of measures k_{Deg} vs I_0) is $k_{Deg} = 3.20 \times 10^{-7}$ M s^{-1} for $I_0 = 4.09 \times 10^{-8}$ mol s^{-1} cm^{-2}: because $q = 9.47 \times 10^{-2}$ s^{-1} and the minimum value is $C_B(t) = 3.38 \times 10^{-5}$ M. For this reason, starting from $C_0 = 2 \times 10^{-4}$ M, we never exceeded the conversion of more than 80% of the initial substrate. According to reaction 2,HCOOH + O_2 → 2CO_2 + 2H_2O, the oxygen demand for 80% of the initial substrate conversion is 8×10^{-5} M. The water oxygen solubility at room temperature is $[O_2]_w = 2.3 \times 10^{-4}$ M,[16] and so the substrate oxidation will consume only the 35% of the initial dissolved oxygen: furthermore, inside the vessel, the suspension is vigorously stirred and can exchange O_2 with its headspace, which contains at least 3×10^{-4} mol of O_2 (p = 1 atm; T = 298 K). From these considerations, we can state that, from a stoichiometric point of view, O_2 limitations do not occur during substrate removal. Furthermore, in the operating conditions, the dimensionless corrective factor $\psi = \frac{1}{b}\frac{\left[\int_0^b \sqrt{T(z)}\,dz\right]^2}{\int_0^b T(z)\,dz}$ is very close to unity. This aspect is extremely important, because it allowed us to develop the discussion by referring to average volumetric variables with the same equations of those referred to surface properties (see eqs 1 and 5). Recently Calza and co-workers used the KM function to fit the experimental $T(z)$ data for $0.05 \leq C_{Cat}$ (g L^{-1}) ≤ 0.60 and to obtain the specific absorption and scattering coefficients (ε_{Abs}, ε_{Sca} in cm^2 g^{-1}) for aqueous TiO_2 suspensions.[18] Starting from the values that they reported for Evonik P25, we determined the theoretical $T(z)$ KM profile for the unique C_{Cat} value (0.1 g L^{-1}) we used in our work. In these conditions, the KM function is also

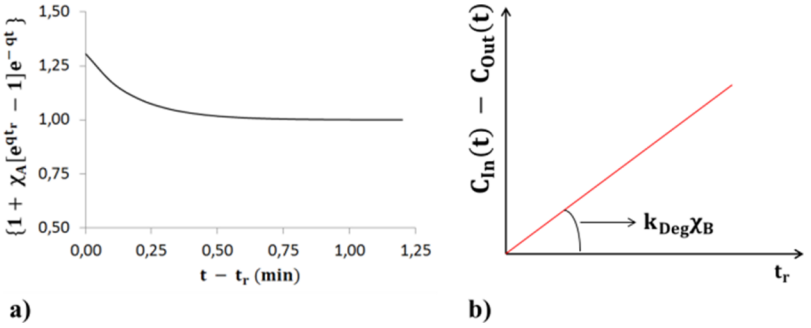

Figure 7. (a) Time-dependent component of eq 14 in the following operating conditions: $\chi_A = 0.38$, $t_r = 17.8$ s, $q = 9.47 \times 10^{-2}$ s^{-1}. (b) Difference concentration inside the illumination chamber is in linear relationship with the residence time when the steady state condition is achieved (i.e. when $\chi_A[e^{qt_r} - 1]e^{-qt} \rightarrow 0$). From eq 15, we obtained that the slope of the line is equal to $k_{Deg}\chi_B$.

https://dx.doi.org/10.1021/acscatal.0c02518
ACS Catal. 2020, 10, 9612−9623

well-approximated by the Lambert−Beer expression (i.e. $T(z) = e^{-\beta z}$), where β (cm^{-1}) is the total extinction coefficient, in which the scattering and absorption contributions are indistinguishable. From these considerations, ψ can be written as

$$\psi = 2\left(\frac{\beta b}{2}\right)^{-1}\frac{[1 - e^{-\beta b/2}]}{[1 + e^{-\beta b/2}]}$$

We determined the β value for our experimental setup by performing a series of measures, varying the spacer (i.e., the thickness of suspension) from 0.1 to 0.4 cm: in each case, the I_0 and $I(b)$ values were determined by filling the illumination chamber with water and with the suspension, respectively. For $C_{Cat} = 0.1$ g L^{-1}, it results in $\beta = 1.512$ cm^{-1}, which is in good agreement with the one evaluated starting from the data reported by Calza et al. ($\beta = 1.619$ cm^{-1}).[18] The corresponding calculated values are $\psi = 0.999$ for $b = 0.1$ cm and $\psi = 0.996$ for $b = 0.3$ cm. This allows us to employ eq 5 as the starting point for the quantitative description of the photocatalytic system under CPI. Furthermore, the evaluation of β allows us to estimate $\overline{\phi_V}$ and to calculate the quantum yield of the photocatalytic process (η): for $I_0 = 4.09 \times 10^{-8}$ mol s^{-1} cm^{-2} (i.e., the value at which CPI experiments are performed) it results in $\eta \cong 0.036$, which is comparable to the value previously reported by Cornu et al.[7] (≈0.021). The fact that for one hundred absorbed photons, only three to four of these are employed in the substrate degradation confirms the great extension of the recombination process and justifies the use of eq 1 (i.e., *recombination regime*) as the starting point for the description of the photocatalytic system. Moreover, this result is perfectly consistent with the observed linear dependence of k_{Deg} versus $\sqrt{I_0}$ (Figure 5). After checking the fundamental hypothesis for the whole model construction, we evaluated τ_L by performing a series of CPI experiments at a fixed duty cycle ($\gamma = 0.2$) and varying t_{ON}: in this way, overfitting problems are avoided because the fitting function (eq 6) has only one variable parameter. Through a regression procedure (nonlinear GRG) on the experimental data with the k_{Deg}^{CPI}/k_{Deg} function (eq 6), we obtained $\tau_L = 352$ ms, and so we built the graph in which the theoretical curve is superimposed on the experimental data (Figure 8). The value of *intrinsic degradation rate* used is $k_{Deg} = 3.20 \times 10^{-7}$ M s^{-1} and recorded in the following experimental conditions: $I_0 = 4.09 \times 10^{-8}$ mol s^{-1} cm^{-2}, $b = 0.3$ cm, $\chi_A = 0.38$, and $t_r = 17.8$ s. Because we previously reported that a t_r of nearly 16 s is enough to achieve the steady-state condition for charge carrier concentration, the k_{Deg}^{CPI}/k_{Deg} for $t_{ON} \geq 16$ s is logically fixed to the duty cycle value (0.2) (see points at $\log_{10}(t_{ON}/\tau_L) = 1.65$ and 2.66 in Figure 8), and therefore, no error bars are provided.

For very short t_{ON}, it results in $k_{Deg}^{CPI} = \sqrt{\gamma}\, k_{Deg}$ (Figure 8): taking into account that the system operates in the *recombination regime* (Figure 5), we can write that $\lim_{t_{ON}\to 0} k_{Deg}^{CPI} = k_{Deg}$ ($I_0' = \gamma I_0$): in other words, there is no quantum yield (or photoefficiency) enhancement related to the CPI technique as predicted by the kinetic model and previously demonstrated by other researchers.[7,8] This result seems to be very similar to the case of catalyst surface resonance,[31] when the activation energy for surface reaction is independent of the binding energy between the substrate/product and catalyst surface. In fact, if the k_{Deg}^{CPI}/k_{Deg} values of Figure 8 were plotted against the logarithm of the frequency (f) of the square wave (i.e., $f \propto (t_{ON})^{-1}$), it would be observed as having a close resemblance to the results obtained by Ardagh et al.[31] However, in CPI experiments the temporal

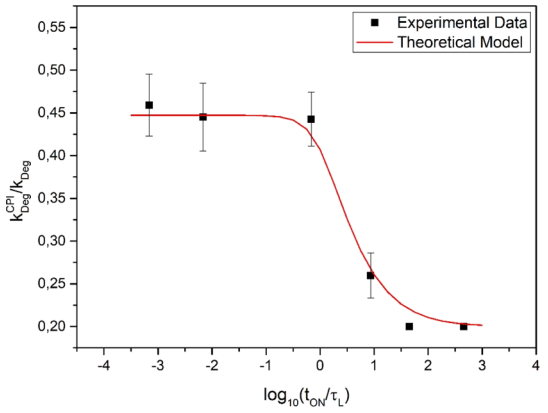

Figure 8. Theoretical model (red curve) and experimental data (black squares) for the ratio between the degradation rate under CPI and continuous illumination versus the base 10 logarithm of the ratio between t_{ON} and τ_L. For the experiments in which $t_{ON} = 240$ μs; 2.4 ms; 240 ms, the operating conditions are: $\chi_A = 0.38$ and $b = 0.3$ cm. For $t_{ON} = 240$ μs, 240 ms, it is $t_r = 17.8$ s, while for $t_{ON} = 2.40$ ms, it is $t_r = 15.9$ s. Error bars account for one standard deviation. The experiment, in which $t_{ON} = 3.05$ s, was performed exploiting the intrinsic periodic illumination due to the photoreactor fluidics (see details in the text).

modulation of the light source determines a change in the surface concentration of active species (i.e., h_s^+, e_s^-); whereas, in the case of catalyst surface resonance, the temporal modulation concerns thermodynamic and kinetic-related properties of the catalyst, which in turn determine the surface concentrations of the substrate and the product.

Figure 8 shows that the change in system behavior occurs between 240 ms and nearly 16 s because for this residence time, we observed a linear relationship between k_{obs} and χ_A. However, the LED source employed in this work cannot provide light pulses on timescales of seconds with $\gamma = 0.2$. Furthermore, for this duty cycle value, a light flash of 3 s implies a period of 15 s, which is comparable with the residence time. In other words, a volumetric element flowing through the illumination chamber would be subjected to only one cycle and could not reach the *two-value condition*. For these reasons, we decided to exploit the intrinsic periodic illumination due to the photoreactor fluidics (see Figure 2) adopting the spacer with $b = 1$ mm and $\chi_A = 0.2$: for $F = 95$ mL min^{-1}, we obtained a $t_r = t_{ON} = 2.84$ s. In this case, k_{Deg}^{CPI} was simply estimated as the slope of the linear relationship $[C_0 - C_B(t)]$ versus t. We obtained $k_{Deg}^{CPI} = (1.08 \pm 0.11) \times 10^{-7}$ M s^{-1}. Moreover, because k_{Deg} is dependent on the thickness of the irradiated suspension (eq 2), a new reference in continuous illumination for $b = 1$ mm is obtained in the following conditions: $\chi_A = 0.2$ and $F = 17$ mL min^{-1}, from which $t_r \cong 16$ s. Both the experiments were carried out at the same incident photonic flux previously reported ($I_0 = 4.09 \times 10^{-8}$ mol s^{-1} cm^{-2}). For the continuous experiment, we measured $k_{Deg} = (4.17 \pm 0.32) \times 10^{-7}$ M s^{-1}. It implies that for $t \geq 2.5t_r$, the difference concentration also becomes independent of the irradiation time (eq 15) in these operating conditions. In this case, with $q = 7.83 \times 10^{-2}$ s^{-1}, in order to refer to the illumination chamber with a unique value for substrate concentration, the degradation can be performed until $C_B = 5.33 \times 10^{-5}$ M (i.e., ≅26.5% of the total initial substrate), which is definitely lower than the value we recorded for the last sampling time ($C_B = 1.07 \times 10^{-4}$ M). It results in $k_{Deg}^{CPI}/k_{Deg} = 0.260$. However, it must be remembered that the k_{Deg}^{CPI}/k_{Deg} function is dependent on $\overline{\phi_V}$ because the modeling parameter m

https://dx.doi.org/10.1021/acscatal.0c02518
ACS Catal. 2020, 10, 9612−9623

is a function of τ_L (see eqs 6 and 7). The mathematical expression for $\overline{\phi_V}$ (mol s^{-1} L^{-1}) is

$$\overline{\phi_V} = 10^3 k I_0 \frac{1}{b} \int_0^b T(z)\, dz \tag{16}$$

Thus, in the dataset from which τ_L has been evaluated (Figure 8), we must take into account that k_{Deg}^{CPI}/k_{Deg} is dependent on the thickness of the irradiated suspension. In the following discussion, the term thickness-dependent is indicated by the subscript "1" or "3" if it refers to the spacer of 1 or 3 mm, respectively. According to the definition of the parameter m (Section 2.2), its expression in the case of b = 1 mm becomes

$$m_1 = [k_{2,v}\overline{\phi_{V,1}}]^{1/2} t_{ON,1} \tag{17}$$

From eq 16, it follows that

$$\overline{\phi_{V,1}} = \overline{\phi_{V,3}} \frac{b_3}{b_1} \frac{[1 - e^{-\beta b_1}]}{[1 - e^{-\beta b_3}]}$$

By substituting the numerical values, we obtain $\overline{\phi_{V,1}} = 1.15\overline{\phi_{V,3}}$: introducing this into eq 17, it results in $m_1 = [k_{2,v}\overline{\phi_{V,3}}]^{1/2}(1.073 \cdot t_{ON,1})$, which is equal to the expression for the parameter m in the case of 3 mm spacer (m_3) with $t_{ON,3} = 1.073 \cdot t_{ON,1}$. In other words, the value of k_{Deg}^{CPI}/k_{Deg} with the 1 mm spacer and t_{ON} = 2.84 s corresponds to the value that we would observe if we performed the test with the 3 mm spacer and t_{ON} = 1.073 × 2.84 = 3.05 s. From the lifetime of active species (τ_L), it is possible to verify the steady-state hypothesis for $[h_s^+]$ in the illumination chamber when the experiment is performed with constant irradiation and $t_r \cong 16$ s. In the worst case, in which for a volumetric element entering the illumination chamber is $[h_s^+] = 0$, the time required to reach 99% of $[h_s^+]_{ss}$ is: $t_{99\%} = \tau_L \tanh^{-1}(0.99) \cong 0.932$ s which implies that only for 5.87% of the residence time, does the $[h_s^+]$ significantly differ from the steady-state value. Furthermore, the time required to remove 90% of charge carriers present in steady-state condition is: $t_{10\%} = 9 \cdot \tau_L \cong 3.17$ s. Taking into account that $t_r^B \cong 25$ s, it implies that substrate degradation process may occur only for 12.67% of the residence time in portion "B" of the photoreactor. Therefore, we have verified the assumptions (1) and (2) made in Section 2.3 to obtain the $C_B(t)$ expression. Cornu et al.[7] observed a similar behavior, in terms of η versus t_{ON}, for the photocatalytic TiO_2 (Degussa P25) oxidation of formic acid under CPI in different experimental conditions, that is, (γ = 0.35, C_{Cat} = 0.006 g L^{-1}, C_0 = 1 × 10^{-4} M, pH = 4.2, $\overline{\phi_V}$ = 2.02 × 10^{-6} mol s^{-1} L^{-1}, and $[O_2]_w$ = 1.3 × 10^{-3} M): they reported a carrier lifetime (toward recombination) of about 100 ms, which is in the same order of magnitude compared with our estimation (≈350 ms). However, for γ = 0.05, they observed two inflections in the curve η versus t_{ON}. The carrier lifetime associated with further transition is 6 ms. The two-transition behavior was reported by the same authors for the TiO_2 bleaching of methyl orange solutions in the stochastic kinetic regime (i.e., a regime in which carrier recombination is minimized), where they found that the illumination time at which η jumps occur are exponential functions of the pH solution.[32] Observed lifetimes are not dependent on the substrate being degraded. Moreover, the fact that they are too long to be those of valence band holes and conduction band electrons suggests that these are consistent with lifetimes of surface-bound species ($O_2^{\bullet-}$ and $HO^{\bullet}$), which may be involved in surface-mediated recombination processes.[32] About this, Ishibashi and co-workers have shown that in the case of TiO_2 anatase films in contact with water solution, under very weak illumination intensity (~0.01 W m^{-2}), superoxide decay obeys pseudo-first-order kinetics with a lifetime of about 70 s. Because the deactivation processes of $O_2^{\bullet-}$ in water solution show second-order kinetics and considering that the lifetime observed is greater that the value expected from the effective rate constant for the disproportionation reactions in which superoxide can be involved in homogeneous solution, they concluded that another decay process exists and the most probable process is the recombination with surface-trapped holes. In addition, they reported that the amount of $O_2^{\bullet-}$ photogenerated is restricted by the number of O_2 adsorption sites rather than light intensity, because adsorbed $O_2^{\bullet-}$ in the case of strong UV light illumination (~150 W m^{-2}) is only 1.6 times the measured value under very weak light intensity.[33] CPI experiments provided consistent results also in the case of gas−solid photocatalytic oxidation of organic compounds. For example, Korovin et al.[8] determined two distinct active species with lifetimes of 30 ms ($HO^{\bullet}$) and 9 s ($O_2^{\bullet-}$) for the TiO_2 (Degussa P25) photocatalytic oxidation of acetone vapor. All these studies highlight that the lifetimes of η (or rate)-determining species in photocatalysis are in the timescale that goes from milliseconds to minutes, which is much greater than that observed for optical signals with ultrafast kinetic spectroscopies (sub-picosecond scale)[34] or in the case of laser flash photolysis experiments (100 ps to 10 ns for charge carriers trapping, 10−100 ns for charge carriers recombination) with the exception of electron transfer to the oxidant (milliseconds).[3] However, the conditions in which these experiments are carried out (i.e., high-power laser irradiation, dilute semiconductor suspensions, or powders) are not representative of the usual conditions prevailing in the photocatalytic degradation of many compounds.[35] The timescales measured from CPI experiments suggest that the intermediates giving rise to the fast transients could be merely precursors of reactive species being transformed at later stages.[32] The experimental results shown in Figure 5 prove that the degradation rate is a function of a generic active species (h_s^+), whose concentration depends on the square root of the incident photonic flux. However, because $\eta \sim 3.6\%$, the lifetime of the active species is determined by the recombination process with a negatively charged surface species (e_s^-) of around equal concentration; therefore, disregarding electron transfer to adsorbed O_2 does not invalidate the model developed in Section 3. Taking into account the expression for k_{Deg} (eq 3), $(h_s^+)_{ss}$ (eq 4), and τ_L (eq 7) developed in the framework of the kinetic model, the following equality can be written

$$k_{Deg} \cdot \tau_L = \frac{k_{3,v}}{k_{2,v}} \tag{18}$$

which can properly be considered as a photocatalytic activity index (PAI) because it is the ratio between the (volume-defined) kinetic constants for substrate TiO_2 electron transfer and for surface recombination. Because τ_L was evaluated from measurements at I_0^{CPI} = 4.09 × 10^{-8} mol s^{-1} cm^{-2}, the k_{Deg} used for PAI estimation is k_{Deg} = 3.20 × 10^{-7} M s^{-1} (i.e., the value measured for continuous illumination at I_0 = 4.09 × 10^{-8} mol s^{-1} cm^{-2}). We obtained PAI = 1.13 × 10^{-7} M. It is important to highlight that: (1) PAI ($k_{Deg} \cdot \tau_L$) evaluation (in contrast with η determination) does not require photoreactors designed to perform actinometric measurements (see Cornu et al.[7,32])

https://dx.doi.org/10.1021/acscatal.0c02518
ACS Catal. 2020, 10, 9612−9623

because photon flux absorbed data are not necessary; (2) $k_{2,v}$ and $k_{3,v}$ are both independent of the type of illumination (CPI or continuous) and of the regime in which the photocatalyst is operating (stochastic, recombination or diffusion-control), and their ratio can be employed also in different conditions from that required for its evaluation (recombination regime); (3) because PAI is not a function of $\overline{\phi_V}$, it could be used to compare photocatalysts with different optical properties. Lastly, considering that $k_{2,v} = k_{2,s}/(C_{Cat}S)$, $k_{3,v} = k_{3,s}\sigma_s'$, and starting from the PAI expression, we can write the homologous surface-defined PAIs

$$\text{PAIs} = \frac{k_{3,s}}{k_{2,s}} = \frac{k_{Deg}\cdot\tau_L}{C_s} \tag{19}$$

where C_s (M) = $C_{Cat}S\sigma_s'$ is the volumetric concentration of substrate adsorption sites. According to the kinetic model, the zero order toward aqueous substrate concentration can be explained by only assuming the total coverage for substrate adsorption sites. Consequently, σ_s' is evaluated by the difference between analytical concentration (i.e., the substrate concentration calculated from the known values of total volume suspension loaded in the photoreactor and the substrate concentration in the stock solution) and measured concentration for the "zero-time" of the experiment (after dark adsorption equilibrium, see Section 2.2). We obtain σ_s' = 5.26 × 10^{-6} mol m^{-2}, from which C_s = 2.89 × 10^{-5} M: so, the PAI value is PAIs = $k_{3,s}/k_{2,s} \cong 4 \times 10^{-3}$. From our point of view, this is the most important result of the work because we have evaluated the ratio between the (surface-defined) kinetic constant for substrate oxidation and surface recombination, which is undoubtedly related to the photocatalyst activity and independent of various experimental conditions such as irradiance, catalyst concentration, substrate concentration, and catalyst specific surface area. Furthermore, the conditions in which PAIs are estimated are those of the irradiation experiments (i.e., the conditions in which the photocatalyst was used). The fact that the (surface-defined) kinetic constant for surface recombination is approximately 250 times the kinetic constant for substrate oxidation is perfectly consistent with the low quantum yield observed ($\eta \cong 0.036$): we want to highlight this aspect because PAIs and η estimations are provided in independent ways.

4. CONCLUSIONS

This work is a further proof that the CPI technique is unable to increase the quantum yield (or photoefficiency) of the photocatalytic process, because for $t_{ON} \to 0$ (the best case) the degradation rate under CPI conditions is equal to that observed for continuous illumination at the same average incident photonic flux. The theory of intermittent illumination, originally developed to describe homogeneous polymerization processes, can be applied very well in the quantitative representation of a heterogeneous photocatalytic system operating in the recombination regime because mass transfer limitations do not occur. As highlighted for the surface-defined PAIs, CPI technique, coupled with the kinetic modeling, allows the evaluation of important parameters, which are not accessible through other experimental procedures. Speculations about the magnitude of these constants pervade the literature because of their importance in understanding the process and for the design of improved catalysts and more efficient procedures for pollutant abatement.

■ ASSOCIATED CONTENT

Supporting Information

The Supporting Information is available free of charge at https://pubs.acs.org/doi/10.1021/acscatal.0c02518.

Instrumental apparatus and degradation tests (PDF)

■ AUTHOR INFORMATION

Corresponding Authors

Marco Prozzi − *Dipartimento di Chimica, Università di Torino, 10125 Torino, Italy*; Email: marco.prozzi@unito.it

Francesco Pellegrino − *Dipartimento di Chimica, Università di Torino, 10125 Torino, Italy; JointLAB UniTo-ITT, 10135 Torino, Italy*; orcid.org/0000-0001-6126-0904; Email: francesco.pellegrino@unito.it

Authors

Fabrizio Sordello − *Dipartimento di Chimica, Università di Torino, 10125 Torino, Italy*; orcid.org/0000-0003-4578-2694

Simone Barletta − *Dipartimento di Chimica, Università di Torino, 10125 Torino, Italy*

Marco Zangirolami − *Fonderia Mestieri Srl, 10093 Turin, Italy*

Alessandra Bianco Prevot − *Dipartimento di Chimica, Università di Torino, 10125 Torino, Italy*

Valter Maurino − *Dipartimento di Chimica, Università di Torino, 10125 Torino, Italy; JointLAB UniTo-ITT, 10135 Torino, Italy*

Complete contact information is available at: https://pubs.acs.org/10.1021/acscatal.0c02518

Notes

The authors declare no competing financial interest.

■ ACKNOWLEDGMENTS

The authors acknowledge funding from Project O, European Union's Horizon 2020 Research and Innovation Programme under grant agreement no. 776816.

■ GLOSSARY

CPI	controlled periodic illumination
I_0	incident photonic flux at the top of the slurry during a continuous illumination experiment (mol s^{-1} cm^{-2})
I_0^{CPI}	incident photonic flux at the top of the slurry during the light pulse of a CPI experiment (mol s^{-1} cm^{-2})
t_{ON}	light flash length of the CPI experiment (s), see Figure 1
t_{OFF}	dark interval length of the CPI experiment (s), see Figure 1
P	period of the CPI experiment (s)
γ	duty cycle, the fraction of the period in which the reaction cell is exposed to the constant photonic flux (I_0^{CPI}) in CPI experiment (a-dimensional)
$k_{i,s}$	surface-defined kinetic constant for surface recombination (i = 2), substrate oxidation (i = 3) and oxidant reduction (i = 4) (m^2 mol^{-1} s^{-1}), see Figure 4
$k_{2,v}$	volume-defined kinetic constant for surface recombination (M^{-1} s^{-1})
$k_{3,v}$	volume-defined kinetic constant for substrate oxidation (s^{-1})
σ_s'	moles of substrate adsorption sites per unit surface area of the catalyst (mol m^{-2})
C_s	volumetric concentration of substrate adsorption sites (M)
C_{Cat}	photocatalyst loading (g L^{-1})

https://dx.doi.org/10.1021/acscatal.0c02518
ACS Catal. 2020, 10, 9612−9623

S photocatalyst specific surface area ($m^2\ g^{-1}$)
$T(z)$ transmittance of the suspension at a distance z from its top (a-dimensional)
b thickness of the irradiated suspension (cm)
$T(b)$ transmittance of the suspension measured at a distance b from its top (i.e., $T(b) = I(b)/I_0$) (a-dimensional)
k absorption coefficient (cm^{-1})
β total extinction coefficient (cm^{-1})
$\{i\}$ surface concentration of species "i" (mol m^{-2})
$[i]$ volumetric concentration of species "i" (M)
ϕ_s rate of radiation absorption per unit surface area of the catalyst (mol s^{-1} m^{-2})
$\overline{\phi_V}$ average photonic flow absorbed per volumetric unit of suspension (mol s^{-1} L^{-1})
η quantum yield (a-dimensional)
k_{Deg} rate of aqueous substrate removal from the illumination chamber (M s^{-1})
k_{obs} rate of aqueous substrate removal from the entire photoreactor (i.e., observed degradation rate) (M s^{-1})
F PP flow (mL min^{-1})
V_i volume of suspension contained in the illumination chamber (i = A) or in the dark part of the photoreactor (i = B) (mL)
V_{tot} total volume of suspension loaded in the photoreactor (mL)
$C_i(t)$ time-dependent aqueous substrate concentration in the illumination chamber (i = A), in the dark part of the photoreactor (i = B) or in the entire photoreactor (i = tot) (M)
C_0 aqueous initial ($t = 0$) substrate concentration (M)
t_r residence time in the illumination chamber (s)
t_r^B residence time in the dark portion of the photoreactor (s)
χ_i suspension volumetric fraction for the illumination chamber (i = A) or the dark part of the photoreactor (i = B) (a-dimensional)
q photoreactor parameter (min^{-1}), see eq [12]
τ_L lifetime of active oxidizing species (s)
PAI photocatalytic activity index (M)
PAIs surface-defined photocatalytic activity index (a-dimensional)
ψ a-dimensional, see text
E_{bg} semiconductor band-gap (J or eV)
r ratio between t_{OFF} and t_{ON} (a-dimensional) m, ratio between t_{ON} and τ_L (a-dimensional)
t time (s)
KM Kubelka–Munk function, see refs 16 and 18
$I(b)$ transmitted photonic flux by the suspension contained in the illumination chamber (mol s^{-1} cm^{-2})

REFERENCES

(1) Fujishima, A.; Zhang, X.; Tryk, D. TiO_2 Photocatalysis and Related Surface Phenomena. *Surf. Sci. Rep.* **2008**, *63*, 515–582.
(2) Bahnemann, D.; Cunningham, J.; Fox, M.; Pelizzetti, E.; Pichat, P.; Serpone, N. In *Aquatic and Surface Photochemistry*; Helz, G. R., Zepp, R. G., Crosby, D. G., Eds.; Lewis Publishing: Boca Raton, 1994; pp 261–316.
(3) Hoffmann, M. R.; Martin, S. T.; Choi, W.; Bahnemann, D. W. Environmental Applications of Semiconductor Photocatalysis. *Chem. Rev.* **1995**, *95*, 69–96.
(4) Sczechowski, J. G.; Koval, C. A.; Noble, R. D. Evidence of Critical Illumination and Dark Recovery Times for Increasing the Photoefficiency of Aqueous Heterogeneous Photocatalysis. *J. Photochem. Photobiol., A* **1993**, *74*, 273–278.
(5) Mehta, D. S.; Saxena, K.; Dubey, S. K.; Shakher, C. Coherence Characteristics of Light-Emitting Diodes. *J. Lumin.* **2010**, *130*, 96–102.
(6) Chen, H.-W.; Ku, Y.; Irawan, A. Photodecomposition of O-Cresol by Uv-Led/TiO_2 Process with Controlled Periodic Illumination. *Chemosphere* **2007**, *69*, 184–190.
(7) Cornu, C. J. G.; Colussi, A. J.; Hoffmann, M. R. Quantum Yields of the Photocatalytic Oxidation of Formate in Aqueous TiO_2 suspensions under Continuous and Periodic Illumination. *J. Phys. Chem. B* **2001**, *105*, 1351–1354.
(8) Korovin, E.; Selishchev, D.; Besov, A.; Kozlov, D. Uv-Led Tio2 Photocatalytic Oxidation of Acetone Vapor: Effect of High Frequency Controlled Periodic Illumination. *Appl. Catal., B* **2015**, *163*, 143–149.
(9) Tokode, O. I.; Prabhu, R.; Lawton, L. A.; Robertson, P. K. J. Effect of Controlled Periodic-Based Illumination on the Photonic Efficiency of Photocatalytic Degradation of Methyl Orange. *J. Catal.* **2012**, *290*, 138–142.
(10) Tokode, O.; Prabhu, R.; Lawton, L. A.; Robertson, P. K. J. Mathematical Modelling of Quantum Yield Enhancements of Methyl Orange Photooxidation in Aqueous TiO_2 Suspensions under Controlled Periodic Uv Led Illumination. *Appl. Catal., B* **2014**, *156–157*, 398–403.
(11) Tokode, O.; Prabhu, R.; Lawton, L. A.; Robertson, P. K. J. Controlled Periodic Illumination in Semiconductor Photocatalysis. *J. Photochem. Photobiol., A* **2016**, *319–320*, 96–106.
(12) Cheremisinoff, N. P.; Rosenfeld, P. E. *Handbook of Pollution Prevention and Cleaner Production*; Elsevier, 2010; p 368.
(13) Pellegrino, F.; De Bellis, N.; Ferraris, F.; Prozzi, M.; Zangirolami, M.; Petriglieri, J. R.; Schiavi, I.; Bianco-Prevot, A.; Maurino, V. Evaluation of the Photocatalytic Activity of a Cordierite-Honeycomb-Supported TiO_2 Film with a Liquid-Solid Photoreactor. *Molecules* **2019**, *24*, 4499.
(14) Preočanin, T.; Kallay, N. Point of Zero Charge and Surface Charge Density of TiO_2 in Aqueous Electrolyte Solution as Obtained by Potentiometric Mass Titration. *Croat. Chem. Acta* **2006**, *79*, 95–106.
(15) Pellegrino, F.; Pellutiè, L.; Sordello, F.; Minero, C.; Ortel, E.; Hodoroaba, V.-D.; Maurino, V. Influence of Agglomeration and Aggregation on the Photocatalytic Activity of TiO_2 Nanoparticles. *Appl. Catal., B* **2017**, *216*, 80–87.
(16) Minero, C.; Vione, D. A Quantitative Evalution of the Photocatalytic Performance of TiO_2 Slurries. *Appl. Catal., B* **2006**, *67*, 257–269.
(17) Minero, C.; Catozzo, F.; Pelizzetti, E. Role of Adsorption in Photocatalyzed Reactions of Organic Molecules in Aqueous Titania Suspensions. *Langmuir* **1992**, *8*, 481–486.
(18) Calza, P.; Minella, M.; Demarchis, L.; Sordello, F.; Minero, C. Photocatalytic Rate Dependence on Light Absorption Properties of Different TiO_2 Specimens. *Catal. Today* **2020**, *340*, 12–18.
(19) Upadhya, S.; Ollis, D. F. Simple Photocatalysis Model for Photoefficiency Enhancement Via Controlled Periodic Illumination. *J. Phys. Chem. B* **1997**, *101*, 2625–2631.
(20) Brandi, R. J.; Alfano, O. M.; Cassano, A. E. Evaluation of Radiation Absorption in Slurry Photocatalytic Reactors. 1. Assessment of Methods in Use and New Proposal. *Environ. Sci. Technol.* **2000**, *34*, 2623–2630.
(21) Brandi, R. J.; Alfano, O. M.; Cassano, A. E. Evaluation of Radiation Absorption in Slurry Photocatalytic Reactors. 2. Experimental Verification of the Proposed Method. *Environ. Sci. Technol.* **2000**, *34*, 2631–2639.
(22) Burnett, G. M.; Melville, H. W. Propagation and Termination Coefficients for Vinyl Acetate Photopolymerization. *Nature* **1945**, *156*, 661.
(23) Bartlett, P. D.; Swain, C. G. The Absolute Rate Constants in the Polymerization of Liquid Vinyl Acetate. *J. Am. Chem. Soc.* **1945**, *67*, 2273–2274.
(24) *Technique of Organic Chemistry*, 2nd ed.; Friess, S. L., Weissberger, A., Eds.; Interscience Publishers, 1953; Vol. *8*, pp 138–145.

https://dx.doi.org/10.1021/acscatal.0c02518
ACS Catal. 2020, 10, 9612–9623

(25) Emeline, A. V.; Ryabchuk, V.; Serpone, N. Factors Affecting the Efficiency of a Photocatalyzed Process in Aqueous Metal-Oxide Dispersions. *J. Photochem. Photobiol., A* **2000**, *133*, 89−97.
(26) Berthoud, A.; Bellenot, H. Recherches Sur La Réaction Photochimique Du Brome Ou De L'iode Avec L'oxalate De Potassium. *Helv. Chim. Acta* **1924**, *7*, 307−324.
(27) Bateman, L.; Gee, G. The Determination of Absolute Rate Constants in Olefinic Oxidations. *Proc. R. Soc. London, Ser. A* **1948**, *195*, 391−402.
(28) Bolland, J. L. Kinetics of Olefin Oxidation. *Q. Rev., Chem. Soc.* **1949**, *3*, 1.
(29) Burnett, G. M. Rate Constants in Radical Polymerisation Reactions. *Q. Rev., Chem. Soc.* **1950**, *4*, 292.
(30) Minero, C.; Bedini, A.; Minella, M. On the Standardization of the Photocatalytic Gas/Solid Tests. *Int. J. Chem. React. Eng.* **2013**, *11*, 717−732.
(31) Ardagh, M. A.; Abdelrahman, O. A.; Dauenhauer, P. J. Principles of Dynamic Heterogeneous Catalysis: Surface Resonance and Turnover Frequency Response. *ACS Catal.* **2019**, *9*, 6929−6937.
(32) Cornu, C. J. G.; Colussi, A. J.; Hoffmann, M. R. Time Scales and Ph Dependences of the Redox Processes Determining the Photocatalytic Efficiency of TiO_2 nanoparticles from Periodic Illumination Experiments in the Stochastic Regime. *J. Phys. Chem. B* **2003**, *107*, 3156−3160.
(33) Ishibashi, K.-i.; Fujishima, A.; Watanabe, T.; Hashimoto, K. Generation and Deactivation Processes of Superoxide Formed on TiO_2 film Illuminated by Very Weak Uv Light in Air or Water. *J. Phys. Chem. B* **2000**, *104*, 4934−4938.
(34) Colombo, D. P.; Bowman, R. M. Femtosecond Diffuse Reflectance Spectroscopy of TiO_2 Powders. *J. Phys. Chem.* **1995**, *99*, 11752−11756.
(35) Grela, M. A.; Colussi, A. J. Kinetics of Stochastic Charge Transfer and Recombination Events in Semiconductor Colloids. Relevance to Photocatalysis Efficiency. *J. Phys. Chem.* **1996**, *100*, 18214−18221.

https://dx.doi.org/10.1021/acscatal.0c02518
ACS Catal. 2020, 10, 9612−9623